Meteorological Studies With the Phased Array Weather Radar and Data Assimilation Using the Ensemble Kalman Filter

Tian-You Yu
University of Oklahoma, 202 West Boyd, rm 427, Norman, OK 73019
phone: (405) 325-3344 fax: (405) 325-7066 email: tyu@ou.edu

Ming Xue
University of Oklahoma, 120 David Boren Blvd, Norman, OK 73072
phone: (405) 325-6561 fax: (405) 325-7689 email: mxue@ou.edu

Mark Yeary
University of Oklahoma, 202 West Boyd, rm 412, Norman, OK 73019
phone: (405) 325-4748 fax: (405) 325-7066 email: yeary@ou.edu

Robert Palmer
University of Oklahoma, 120 David Boren Blvd, rm 4614, Norman, OK 73072
phone: (405) 325-6319 fax: (405) 325-7689 email: rpalmer@ou.edu

Sebastian Torres
University of Oklahoma, 120 David Boren Blvd, rm 4921, Norman, OK 73072
phone: (405) 325-6633 fax: (405) 325-6783 email: sebas@ou.edu

Michael Biggerstaff
University of Oklahoma, 120 David Boren Blvd, Norman, OK 73072
phone: (405) 325-3881 fax: (405) 325-7689 email: drdoppler@ou.edu

N00014-06-1-0590
Team's Project Website: http://arrc.ou.edu/depscor

LONG-TERM GOALS

The long-term goal of this project is to integrate two state-of-the-art technologies, the phased array weather radar (PAR) and the emerging Ensemble Kalman Filter (EnKF) data assimilation method, to optimize the radar performance and improve coastal and marine numerical weather prediction (NWP).

OBJECTIVES

This project leverages on the new PAR in Norman, Oklahoma to exploit phased array technology and its applications to improve NWP through EnKF data assimilation with the goal of improving environmental characterization and forecast to optimize naval operation. This project will further enhance the existing collaboration among ONR, National Serve Storms Laboratory (NSSL), and the University of Oklahoma (OU) to achieve the four specific research objectives: (1) develop an EnKF framework for optimally assimilating quantitative observations of the atmosphere including the PAR data, (2) design a sophisticated radar emulator which will be used to validate innovative processing techniques developed in the project and to design accurate and efficient forward observation operators

Report Documentation Page

Form Approved
OMB No. 0704-0188

1. REPORT DATE	2. REPORT TYPE	3. DATES COVERED
30 SEP 2008	**Annual**	**00-00-2008 to 00-00-2008**

4. TITLE AND SUBTITLE	
Meteorological Studies With The Phased Array Weather Radar And Data Assimilation Using The Ensemble Kalman Filter	5a. CONTRACT NUMBER
	5b. GRANT NUMBER
	5c. PROGRAM ELEMENT NUMBER
6. AUTHOR(S)	5d. PROJECT NUMBER
	5e. TASK NUMBER
	5f. WORK UNIT NUMBER
7. PERFORMING ORGANIZATION NAME(S) AND ADDRESS(ES) **University of Oklahoma,202 West Boyd, rm 427,Norman,OK,73019**	8. PERFORMING ORGANIZATION REPORT NUMBER
9. SPONSORING/MONITORING AGENCY NAME(S) AND ADDRESS(ES)	10. SPONSOR/MONITOR’S ACRONYM(S)
	11. SPONSOR/MONITOR’S REPORT NUMBER(S)

12. DISTRIBUTION/AVAILABILITY STATEMENT
Approved for public release; distribution unlimited

13. SUPPLEMENTARY NOTES
code 1 only

14. ABSTRACT
The long-term goal of this project is to integrate two state-of-the-art technologies, the phased array weather radar (PAR) and the emerging Ensemble Kalman Filter (EnKF) data assimilation method, to optimize the radar performance and improve coastal and marine numerical weather prediction (NWP).

15. SUBJECT TERMS

16. SECURITY CLASSIFICATION OF:			17. LIMITATION OF ABSTRACT	18. NUMBER OF PAGES	19a. NAME OF RESPONSIBLE PERSON
a. REPORT	b. ABSTRACT	c. THIS PAGE			
unclassified	**unclassified**	**unclassified**	**Same as Report (SAR)**	**14**	

Standard Form 298 (Rev. 8-98)
Prescribed by ANSI Std Z39-18

for assimilating PAR data, (3) advance phased array radar technology through the development of novel signal processing techniques and integration of current state-of-the-art technologies to provide high-quality and high-resolution weather measurements, and (4) evaluate the impact of scanning strategies including SPY-1 tactical and non-tactical waveforms on data assimilation and NWP using the Observing System Simulation Experiments (OSSE) and Observing System Experiments (OSE). Optimal scanning strategies of PAR for NWP model initialization will be developed and tested.

APPROACH

Our multidisciplinary team is comprised of scientists with academic and industrial expertise in radar engineering, radar signal processing, EnKF data assimilation, numerical modeling, and weather prediction. Our approach is to exploit these complementary talents to achieve the goals of the proposed research. The five main research thrusts are discussed in the following.

(1) **Design of the PAR Emulator**: A sophisticated PAR emulator is designed to take in high-resolution three-dimensional meteorological fields and to generate synthetic radar time series data. The output of the emulator is then processed to produce the three spectral moments (reflectivity, mean radial velocity and spectrum width). The emulator is flexible enough to produce radar data for various waveforms, sensitivity, and sectoring. The emulator will serve as a vehicle for developing accurate and efficient forward observation operators for PAR data assimilation. Moreover, error characterization can be obtained in the emulation and will be fed into the EnKF system.

(2) **Establish the EnKF system**: The existing EnKF-based OSSE framework for radar data developed by our group will be extended (a) to use much more realistic, yet efficient, forward observation operators that will be derived from the full-scale PAR emulator discussed in (1), (b) to handle PAR data collected in various non-conventional manner such as angular oversampling, and (c) to effectively account for model errors. The availability of an accurate and realistic radar emulator will allow us and the Navy to evaluate the impact of various simplifications (needed for efficient) in the observation operator on the quality of analysis and the subsequent forecast.

(3) **Technology Innovation**: This research thrust focuses on the exploration of phased array technology merged with novel signal processing techniques. An agile beam phased array radar has the potential to not only increase the scanning rate, but also to measure meteorological variables not currently available and to enhance data quality. For example, a novel scanning scheme termed beam multiplexing (BMX) is developed to optimize the scan time and data quality. In addition, the refractivity on surface, which can serve as a proxy of humidity, can be measured from the radar returns from ground clutter. The impact of these technology innovations on numerical prediction can be evaluated and quantified using the OSSE and OSE.

(4) **Observing System Simulation Experiment (OSSE):** A comprehensive simulation system is being designed to integrate the processes of designing radar scanning strategies, making observations, assimilating data, and producing forecasts with the goal of improving short-term weather prediction and better understanding the relationships among all involved processes. The SPY-1 waveform with 1-pulse (reflectivity only) in clear mode, 3- or 4-pulse in Moving Target Indicator (MTI) mode, 16-pulse, and 32-pulse will be simulated and their impact on data assimilation and weather forecasting will be evaluated and quantified. Moreover, a framework for developing an optimal scanning strategy is being established based on a feedback design in the simulation. In other words, the information of the

difference between the forecast and high-resolution model outputs can be used to adjust scanning patterns until optimal results are achieved.

(5) **Data Collection and Observing System Experiments (OSE):** The findings and lessons learned through radar emulator and OSSEs will then be demonstrated using the PAR at NWRT. Various scanning strategies tested with the OSSEs will be implemented with the PAR. We will leverage on a suite of existing weather radars including the research NEXRAD (KOUN), the mobile SMART radars, the nearby operational NEXRAD (KTLX) radar to validate the PAR measurements and retrieved variables.

About the Team: A multidisciplinary team including 6 OU professors and two postdoctoral fellows has been assembled to execute the project. The principal investigator, Prof. Yu is responsible for providing technical expertise and project management, including planning and coordination, monitoring the progress, and reporting to the program manger. Prof. Xue is in charge of data assimilation, numerical models, and NWP. He has been providing the high-resolution model data to be used for the PAR emulation. Prof. Yeary brings his expertise of adaptive signal processing, Kalman filtering, and clutter filtering to develop optimal scanning strategies. Prof. Palmer has been working on the development of PAR emulators and SA algorithms. Prof. Torres who also holds an adjunct faculty position in ECE is involved in the evaluation and quantification of the impact of the PAR scanning strategies on data assimilation and numerical prediction. Prof. Biggerstaff is strongly engaged in the design and coordination field experiments to exercise and validate the results.

WORK COMPLETED

The team has been continuously working toward project goals. The following specific tasks are completed.

(1) **Realization of EnKF Using Real Data**: The major effort of EnKF system this year is focused on the development of an effective multiscale scheme/procedure to significantly improve EnKF analysis and forecast for real cases. The case studied is the tornadic supercell in Oklahoma on May 8, 2003. This case was selected mainly because it was previously investigated and analyzed using the ARPS 3DVAR and cloud analysis (Hu 2005), which can provide a base line for comparisons. In the multiscale approach, EnKF analysis was performed using both 3 km and 1.5 km (1 km for some experiments) horizontal resolutions. For the 3 km EnKF analysis, only mesonet data were used. For the analysis on higher resolution (1 km or 1.5 km), one or two radar data were used, but sometimes mesonet data were also included. However, the inclusion of mesonet data for the EnKF analysis on higher resolution did not show significant improvement and need further investigation. Ensembles on higher resolution were nested on those with the lower resolution. For the initialization of the ensemble on the 3 km resolution, perturbations were generated from the pseudo sounding extracted from the ARPS 3DVAR. Additionally, storm scale perturbations were added to the initial ensembles on the higher resolution.

(2) **Framework for Adaptive Weather Sensing Using Time Balance**: To fully unleash the power of the PAR for adaptive weather sensing, one of the vital components is to schedule multiple tasks that are competing for radar time, such as surveillance and tracking multiple storm cells. For example, one may like to interrogate hazardous or potentially hazardous cells frequently while maintain surveillance task to detect possible new cells. For example, accomplishments have been made by the team to cluster

and identify storm cells within the PAR data (Root et. al. 2009), and efforts are underway to develop real-time tracking algorithms. For a single radar to perform multiple tasks, a algorithm is needed to schedule these tasks in a sequence and to meet the requirement of the update rate for each task. The concept of Time Balance (TB) (Bulter 1998) is introduced to design and schedule scanning strategies for a number of tasks with the goal of providing rapid update of hazardous regions without compromising data quality. TB is a dynamical process that schedules those competing tasks, by balancing the amount of radar time and the time required by each task. In this work, simulated radar data are used to compare the performance of TB-based scanning strategies with the conventional Volume Coverage Pattern (VCP) used in the operational Weather Surveillance Radar- 1988 Doppler (WSR-88D).

(3) **Data Collection and the Development of Interface to the ARPS**: Through our earlier OSSEs (Lei et al. 2008), it has been shown that the azimuthal over-sampling and higher update time of the PAR data can improve the analysis and prediction of convective storms. To further verify these findings, PAR data were collected using angular over-sampling with 0.5^{o} increment in the evening of 17 April 2008 for convective storms. The PAR experiment was carefully designed to match the WSR-88D update time of VCP11 (i.e., 120 sec for 90^{o} azimuthal coverage and from 0.5^{o} to 19.5^{o} in elevation with 31 tilts). In other words, the number of samples available in each radial for the PAR is almost halved compared to the standard sampling of WSR-88D. This special design allows us to assess the trade-off between angular over-sampling and the corresponding increased error in the measurements of reflectivity and velocity for the same update time as WSR-88D. An example of PAR data collected during this experiment is shown and discussed in Figure 4. An interface for the ARPS EnKF system to ingest PAR data with flexible scanning strategies was developed. In the interface, basic quality control including velocity unfolding was included.

(4) **Technology Innovation:** Spectral processing was identified by Fabry and Keeler (2003) as one of the trends in meteorological radar signal processing to enhance accuracy and sensitivity of weather information. A Doppler spectrum offers an additional degree of freedom to exploit the dynamic information within the radar volume, which is not available in time-domain processing such as the autocovariance (pulse-pair processing) method. Moreover, a Gaussian-shaped spectrum is assumed in the autocovariance method, while no prior assumption of the spectrum shape is required in spectral processing. In other words, biases in velocity and spectrum width estimates may result in the autocovariance method if this assumption is violated. The impact of non-Gaussian weather spectra on these biases are formulated and quantified in theory and consequently verified using numerical simulations. Radar Doppler spectra that deviate from a Gaussian shape were observed from a supercell thunderstorm on 10 May 2003, which exhibit features such as dual-peak, flat-top, and wide skirt in the non-tornadic region. These interesting features can be revealed using spectral analysis of raw weather signals. A spectral model of a mixture of two Gaussian components, each defined by its three spectral moments, is introduced to characterize different degrees of deviation from Gaussian shape. A non-linear fitting algorithm was developed to estimate the six spectral moments as well as the noise level of observed Doppler spectra. It was shown via simulations and real data that spectra reconstructed from the dual-Gaussian fitting algorithm can better describe these non-Gaussian spectra than those from the standard autocovariance method. In addition, clutter mitigation that leverages off the sidelobe cancellers of the PAR and multichannel receivers recently funded by the National Science Foundation is developed and studied using simulations. Recent studies have demonstrated that weather radar can measure the refractivity field using ground targets (e.g., Fabry et al. 1997), which can be a good proxy for near-surface humidity field and have the potential to improve prediction of convective storms. An

independent refractivity retrieval algorithm for the PAR was recently developed and demonstrated (Cheong et al. 2008).

RESULTS

The results are highlighted in the following four areas.

(1) **Application of ARPS EnKF to a tornadic supercell on May 8, 2003**

A schematic diagram is shown in Figure 1 to exemplify the multiscale analysis in a benchmark experiment of the May 8 2003 case.

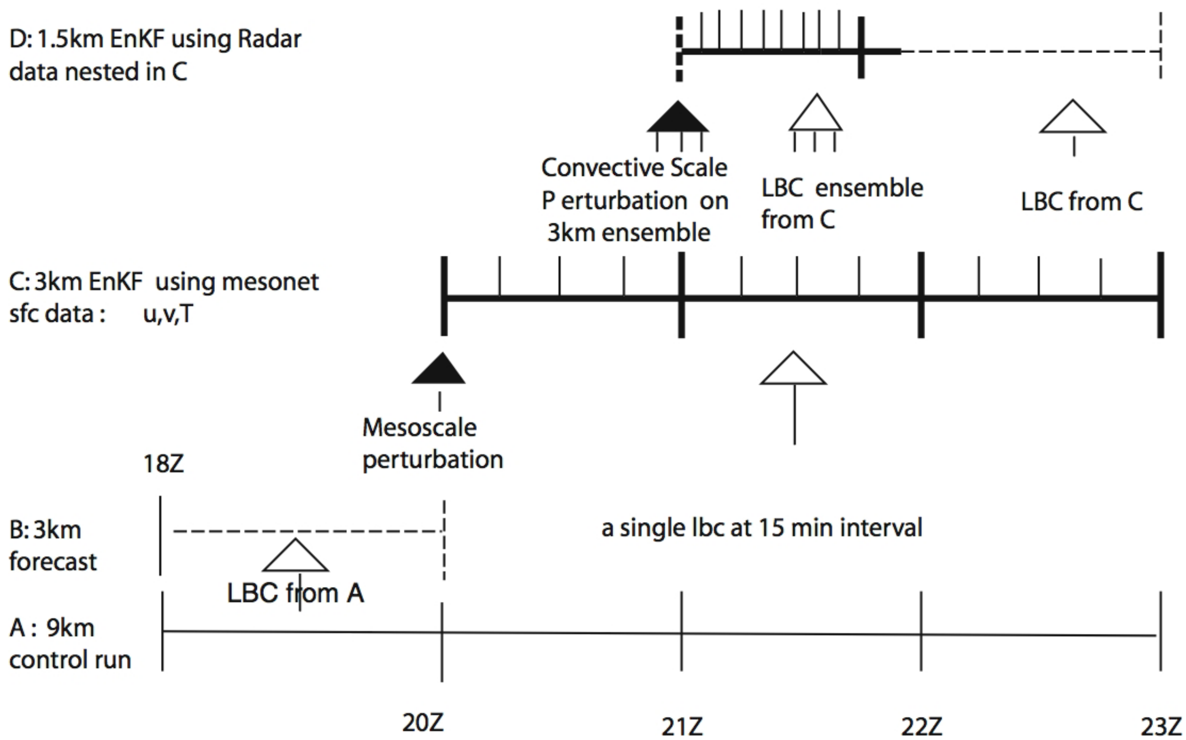

Fig.1, Schematic diagram of the multiscale approach used in the benchmark experiment. From bottom to top, the single 9 km control run in A is the ARPS simulation with initial and lateral boundary conditions (LBC) from Eta. At each hour, the available sounding and surface data are analyzed by the ARPS 3DVARsystem (Hu 2005). The 9 km run provides initial and lateral boundary conditions for the 3 km forecast of B from 18:00 to 20:00UTC, which will be used as the first guess for initial ensemble on 3 km resolution in C.

In the multiscale approach for storm scale EnKF, two important components are described as follows. (a) Analysis was performed on two horizontal resolutions of 3 km and 1.5 km (1 km resolution was used sometimes for other experiments) as indicated by the top two panels of Figure 1C and 1D. The Mesonet data were used for 3 km EnKF and radar data (and sometimes Mesonet data) were used for 1.5 km EnKF analysis. Ensembles in 1.5 km resolution EnKF were nested on those of 3 km resolution. The latter provides initial and lateral boundary conditions (LBC) for the former on a one-to-one basis.

It is found that the analysis of surface Mesonet data on 3 km resolution over the one-hour window (i.e., 20:00—21:00UTC in Figure 1C) prior to the analysis on 1.5 km resolution (i.e., 21:00 to 22:45UTC Figure 1D) can significantly improve the lower level wind fields in the initial ensembles of the later. (b) For the initialization of the ensembles on 3 km EnKF, perturbations that are representative of mesoscale forecast errors for each member were generated by the ARPS 3DVAR with inputs of perturbed pseudo soundings and the first guess from previous forecast fields (from Figure 1B to 1C). The pseudo soundings were also extracted from the first guess. These representative mesoscale forecast errors are required for the EnKF analysis of the mesonet data in Figure 1C.

In this benchmark experiment, the EnKF of Mesonet data on 3 km resolution was performed from 20:00 to 23:00UTC every 15 min. On 1.5 km resolution, two WSR-88Ds of KTLX and KFDR were analyzed from 21:05 to 21:45UTC every 5 min. Initiated from the analyzed ensemble mean of 1.5 km EnKF at 21:45UTC, the forecast was performed for one hour on the same resolution. As shown in Figure 2, the basic structure of the supercell storm is well captured in the forecast of this benchmark experiment. More importantly, the supercell storm is well maintained through the entire forecast period. In the upper right panel of Figure 2, it is evident that the updraft in accordance with the major vertical vorticity center is still rather strong and clear at 22:45 UTC, the final forecast time. The 30-min and 60-min forecast reflectivity at elevation of 0.48^{o} are presented in the bottom left and right panels of Figure 3, respectively. The observed fields of KTLX radar reflectivity from the same time period and elevation angle are presented on the upper two panels. It is clear that the forecast storm is generally consistent with the observations. Nevertheless, it is also apparent that the position of forecast storm is on average approximately 10-20 km off from the observations and spurious cells exist mainly on the southwest and north of the storm. Note that some spurious cells are outside the domains in Figures 2 and 3 and therefore are not shown.

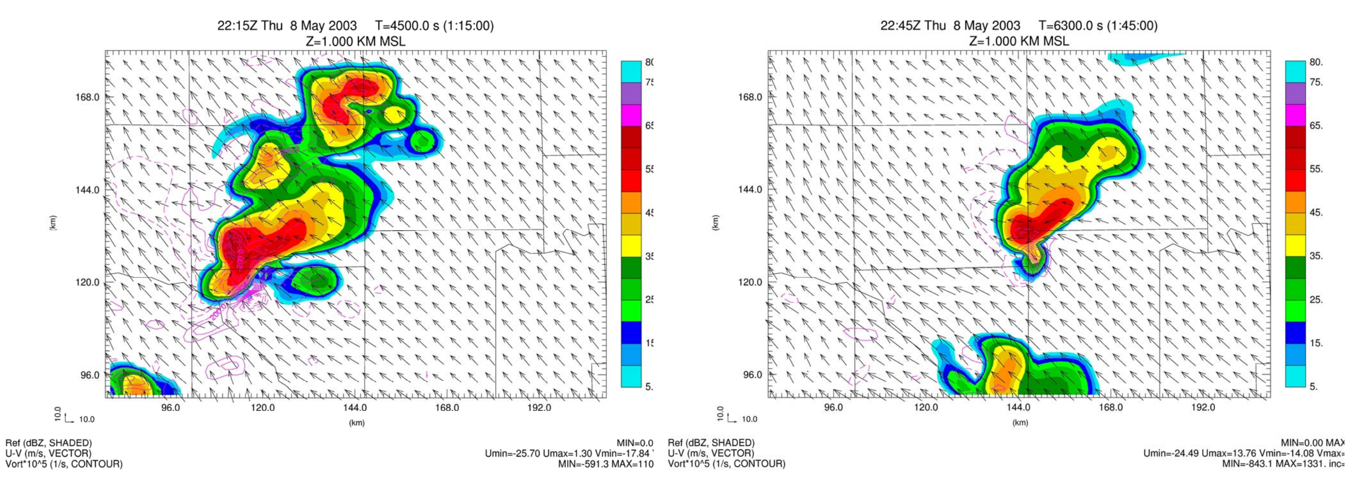

Figure 2: Forecast reflectivity (color shaded), storm-relative wind field (vector), vertical vorticity (contour) at 1 km MSL and from 30 min (left panel) and 60 min (right panel) for the benchmark experiment, initiated from analyzed ensemble mean at 21:45UTC May 8, 2003.

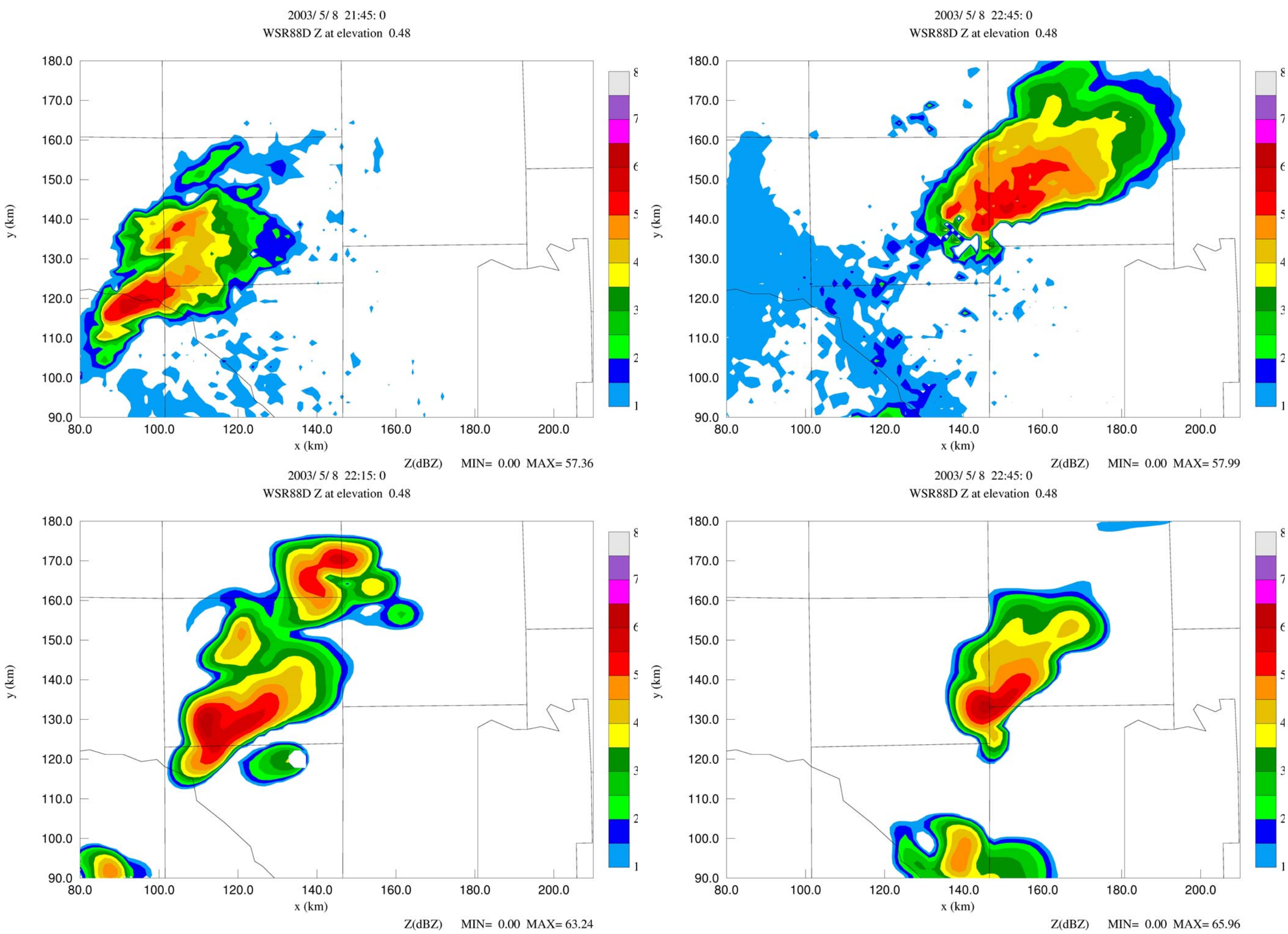

Figure 3: The upper two panels are the KTLX radar reflectivity at the first elevation angle of 0.48^o from 22:15 and 22:45 UTC. The bottom two panels are 30-min and 60-min forecast reflectivity at the corresponding time in the benchmark experiment.

Based on the results of experiments performed so far, the key lessons learned are listed as follows. (a) The inclusion of surface data in 3 km EnKF analysis significantly improves the lower level fields and as a result, more accurate initial fields at lower levels for the ensembles on 1.5 km resolution can be obtained. (b) The multiscale approach provides better representative samples of forecast error than those of conventional storm scale EnKF based on a single resolution. Our results indicate that if only the conventional EnKF method was used on the single higher resolution (ex, 1 km), and the same initial ensemble forecast mean was used as the first guess fields, the analysis is degenerated significantly in first several cycles. Additionally, abnormally strong spurious updraft can be generated and the model becomes unstable. (c) The results of using two radars are, of course, better than those of using one radar. But, our experiment with only the KTLX radar can still produce a storm forecast that is also generally consistent with observation without unrealistic decay (figure is not shown). (d) The impact of EnKF surface data analysis on the higher resolution needs further investigation. Present work doesn't show significant benefits.

(2) **Development of the Framework for Adaptive Weather Sensing**

Our preliminary results of adaptive sensing using time balance (TB) are exemplified in the following figure with the focus of scheduling multiple tasks. The PAR is located at the origin of the upper plot with initially two storm cells (#1 and #2) are presented. It is assumed that the number of radials for each cell and the storm tracks are known and updated from the storm-tracking algorithm. Two tasks of tracking and one task of surveillance are being scheduled. Each tracking task is defined by the occupancy, which is the ratio of dwell time and update time. Surveillance is performed on a randomly radial-by-radial basis over the non-tracking region. An example of how the tasks are scheduled is shown in the middle panel given the number of radials for #1 and #2 are 14 and 18 and the occupancy of cell #1 and #2 is 53% and 27%, respectively. The three tasks are color-coded as follows. Tracking of cell #1 and #2 is denoted by blue and red, respectively and the surveillance is indicated by yellow. The improvement factor (If) is introduced to quantify the performance of scheduling of adaptive sensing, which is defined by the ratio of the observational time on the storm cell using adaptive sensing to the one using WSR-88D's VCP. The dwell time of each tracking task is designed such that the quality of reflectivity and velocity is comparable with the one from VCP11. In addition, for the surveillance region, only 8 pulses are transmitted per radial. Therefore, improvement factor larger than one indicates the cell is revisited more frequently than the VCP11, while the same data quality is maintained. The improvement factors for cell #1 and #2 as a function of total occupancies for tracking are denoted by solid blue and red lines, respectively, on the bottom left panel. It is evident that the improvement factor increases as the occupancy for tracking increases. To further improve the time on the cell using adaptive sensing, it is proposed to implement Beam MultipleXing (BMX) in the elevation direction. The resulted improvement factor is denoted by dashed blue and red lines for cells #1 and #2, respectively. Moreover, a new cell is formed and detected at time t=8.3 sec. The occupancy for the three tracking tasks is subsequently re-assigned. Consequently, the scheduling algorithm will be dynamically adjusted to include the new task (denoted by cyan in the middle panel). The improvement factor for the three cells is shown on the bottom right panel.

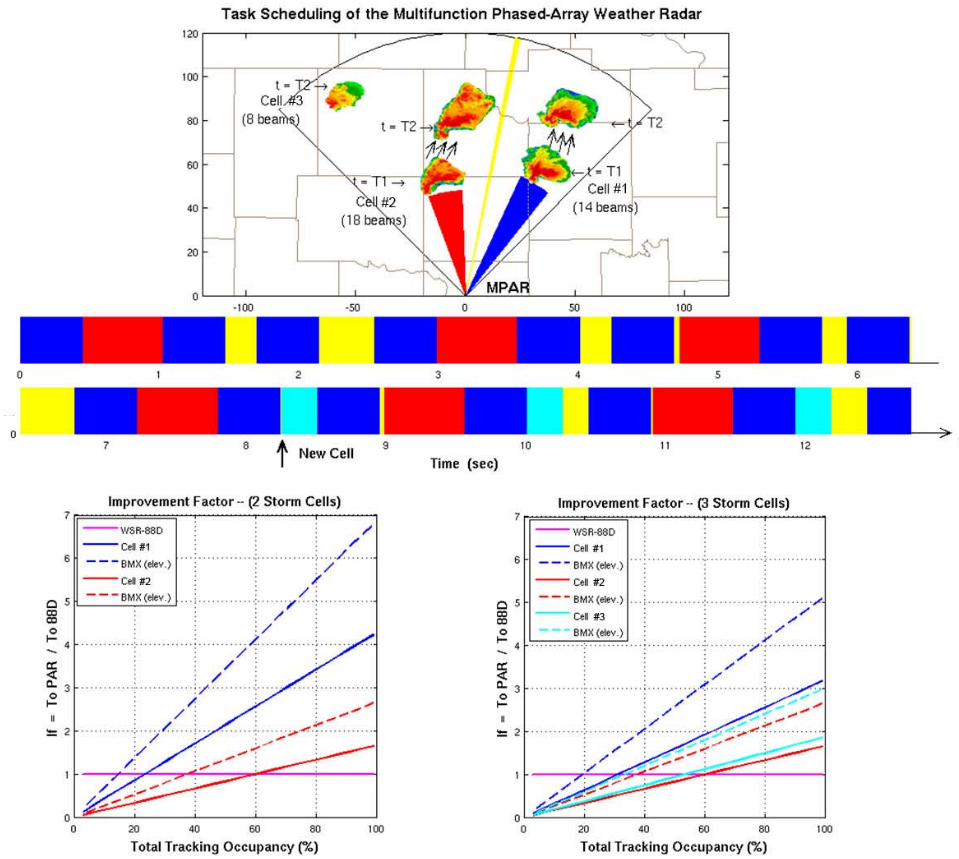

Figure 3: Demonstration of scheduling storm tracking and weather surveillance using time-balance approach. The top panel demonstrate the weather scenario for simultaneous storm tracking and surveillance. The tasks scheduled using TB is exemplified in the middle panel. The performance of TB-based scanning strategy and scheduling are presented on the bottom two panels.

(3) **Data Collection**

The reflectivity field, at 22:30 UTC 17 April 2008, observed by the PAR in the experiment is shown in Figure 1(a). Some line-shaped convective storms accompanying a low-pressure trough were generated over Oklahoma. The PAR, which has 90 degrees coverage in azimuth observed the southwest part of the line-shaped system. Finer scales (~10 km in horizontal) of strong convective cellular precipitations constituting the storm were well expressed by the azimuthal over-sampling data. The system was also observed by the KTLX with 1-degree beam width, which is not oversampling as shown in Figure 1(b). Although the system was observed with wide coverage (360 degrees in azimuth), the inner cellular structures were not well expressed by the KTLX data. The remarkable advantage of the over-sampling of the PAR is shown in a region far from the radar (more than 100 km, the southwest of the radar in figures 1(a), (b)). In addition to the azimuthal over-sampling, high spatial resolution of 27 elevation angles from 0.5 to 19.5 degrees scanning was performed to detect detailed vertical inner structures of storms.

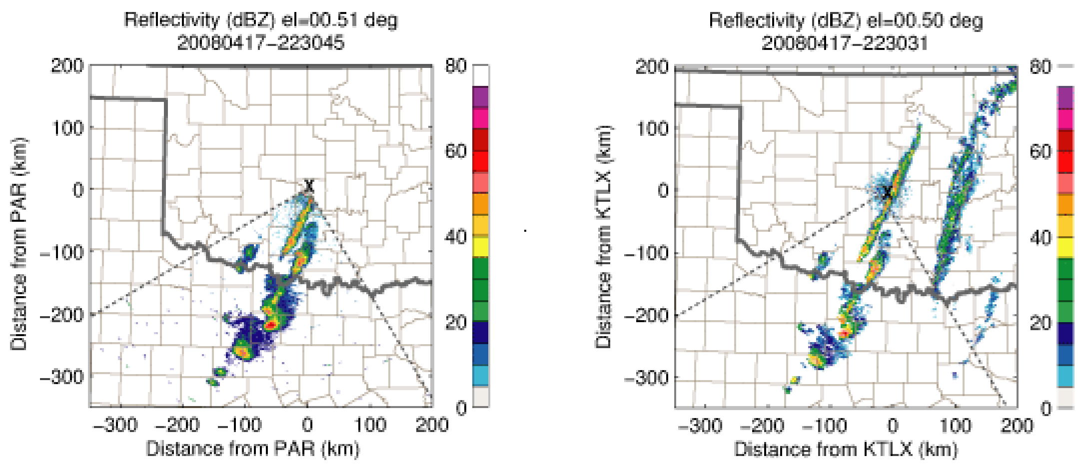

Figure 4: Reflectivity fields at 22:30 UTC April 17 observed by the NWRT PAR with azimuthal over-sampling (left panel) and the KTLX (right panel). Both figures correspond to the lowest elevation of 0.5°. The cross (x) indicates each radar site (the PAR and the KTLX are located at almost same place). The dashed lines in the both figures indicate the 90° azimuthal coverage of the PAR.

(4) **Investigate the Impact of non-Gaussian Weather Spectra on the Bias of Spectral Moments**

In this work, many interesting spectra that deviate from Gaussian are shown from a tornadic supercell observed by the KOUN operated by the National Severe Storms Laboratory (NSSL). In addition, the dual-Gaussian fitting algorithm is applied to these spectra to retrieve the six moments. Although KOUN is not a phased array system, the spectral analysis developed and results obtained in this section can also be applied to the PAR. Time series data from a supercell thunderstorm in central Oklahoma on 10 May 2003 were collected. The autocovariance-processed fields of reflectivity, mean radial velocity, and spectrum width at approximately 0405 UTC are presented from the left to the right columns in Figure 4, respectively. In addition, the top and bottom rows are those fields from elevation angles (ϕ) of 1.5^o and 0.5^o, respectively. Generally speaking, these fields from the two consecutive elevation scans exhibit fair continuity, except for a region of enhanced spectrum widths (>6 m/s) only at the lowest elevation angle of 0.5^o, which appears as a fan shape on the south side of the storm and the northeast of hook echoes. It is observed that the region of enhanced spectrum width is associated with non-Gaussian spectra. Spectra from the region of enhanced spectrum widths are exemplified using those from the azimuthal angle (θ) of 35^o and ranges between 55 to 75 km, that is depicted by the line AB in Figure 4 and are shown in the last column of Figure 5 for two elevation scans.

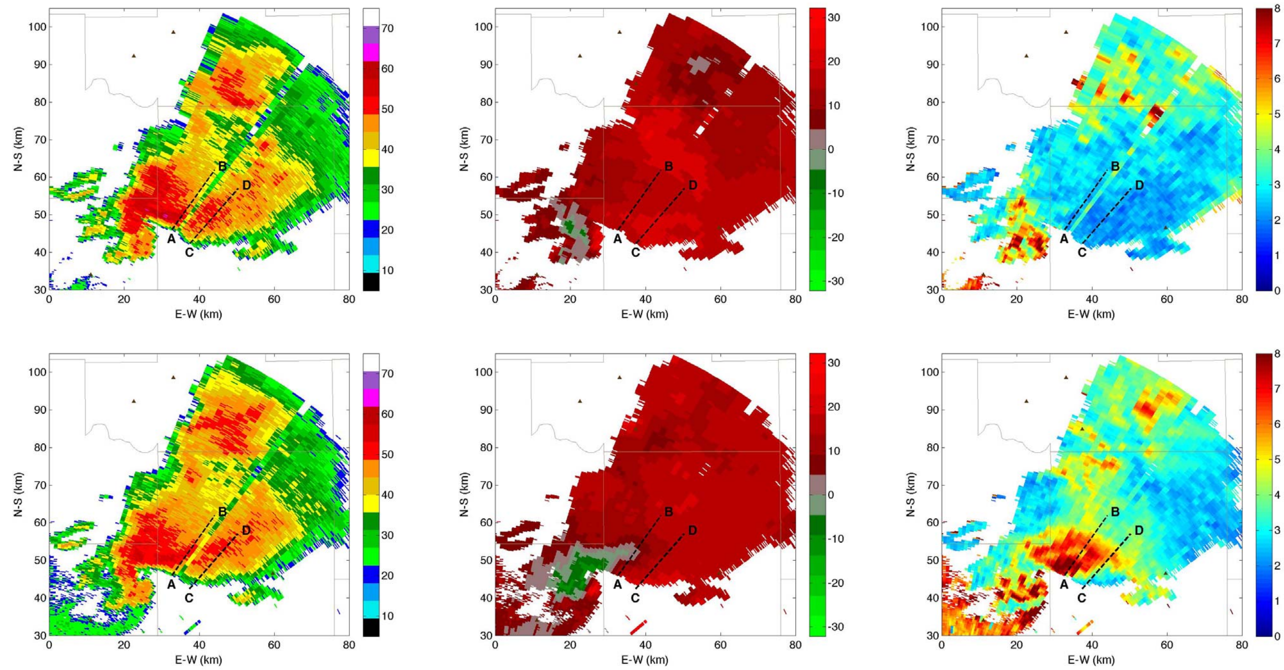

Figure 5: The fields of reflectivity, mean velocity and spectrum width from KOUN radar at the lowest elevation angle of 0.5^o and 0405 UTC 10 May 2003 are shown on the bottom panels from left to right, respectively. Results from the next elevation angle of 1.5^o are presented in the top panels.

At each range gate, a Gaussian-shape spectrum can be reconstructed using the three spectral moments estimated by the autocovariance and is denoted by $\hat{S}_a(v)$. Moreover, the reconstructed spectrum using dual-Gaussian fitting algorithm is denoted by $\hat{S}_d(v)$. Those reconstructed spectra are shown in the first and second columns for the two elevation scans, respectively. Observed spectra shown in the third column are also included and denoted by thick gray line. Note that spectra at ϕ=0.5^o posses signatures of broad spectrum with relatively flat-top or dual-peak pattern and becoming narrower with increasing range. These spectra can be reconstructed by two Gaussians with distinct mean velocities but comparable power. It is also evident that the autocovariance method produce wider spectrum with mean velocities approximately between the locations of the two peaks, as shown in the first column of Figure 5. For the case of ϕ=1.5^o, spectra exhibit signatures of a single dominant peak and sometimes with tails (wider bases) such as those from ranges between 60 km and 68 km. In the dual-Gaussian model, the dominant peak is characterized by a strong and narrow Gaussian component and the tail can be described by the second component with smaller power and larger spectrum width. As a result, the autocovariance method can estimate the mean velocity of the dominant component but has the tendency to overestimate its spectrum width as the tail becomes stronger, as demonstrated by those spectra between of 60 km and 70 km. As spectra become more Gaussian-like between 72 and 76 km, the difference of reconstructed spectra from the autocovariance and dual-Gaussian fitting methods becomes smaller. Another interesting result is that spectra from ϕ=1.5^o overlapped with the right portion of the spectra at ϕ=0.5^o, which can be exemplified by the spectra between 65~km and 70 km as shown in the rightmost column of Figure 5. A hypothesis of vertical shear pattern with enhanced reflectivity structure at lower altitudes was proposed for such transition and was supported by

performing numerical simulations. Detailed results can be found in the recent-accpeted paper of Yu et al. (2008) in the Journal of Atmospheric and Oceanic Technology.

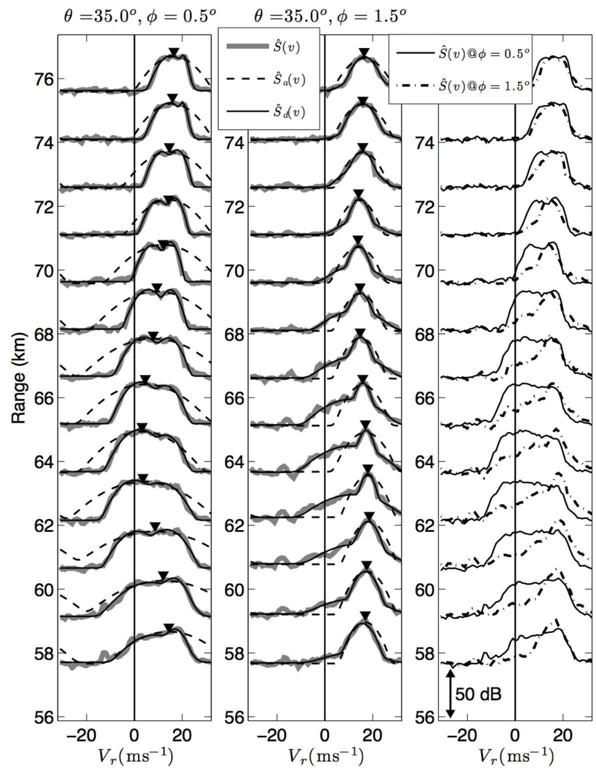

Figure 6: The first and second column are the averaged spectra $\hat{S}(v)$, denoted by thick gray lines, at the azimuth of 35^o for the two consecutive elevation angles, respectively. Observed spectra from ϕ=0.5^o and 1.5^o shown in the first two columns are overlaid in the third column with solid lines denoting spectra at ϕ=0.5^o and dash-dotted lines representing those at 1.5^o. All spectra are shown in a dB scale. The mean velocities estimated by the autocovariance method are denoted by the location of downward triangles.

IMPACT/APPLICATIONS

In storm scale EnKF, one of the challenging issues is that the forecast storm, initiating from the analysis ensemble mean, often decays unrealistically faster than the storm in reality, even when the radar fields (reflectivity and radial velocity) from analysis match well with the ones from observations. This common issue suggests the deficiency in the analysis of unobserved state variables in the existing conventional storm scale EnKF and needs to be addressed before EnKF can be practically applied to real cases using radar data including the PAR. The work of multiscale EnKF have shown promising results for alleviating this issue. Currently, it is used as an effective tool to perform the study of storm scale EnKF for real cases. It is expected that this approach can be used as a framework to advance storm scale EnKF including PAR data.

RELATED PROJECTS

There is no related DoD project.

REFERENCES

Butler, J. M., 1998: Multi-function radar tracking and control, Ph.D. dissertation, University College London, 227 pp.
Fabry, F. and R. J. Keeler: 2003, Innovative signal utilization and processing. Radar and Atmospheric Science: A Collection of Essays in Honor of David Atlas, R. M. Wakimoto and R. C. Srivastava, eds., AMS, Boston, Mass., 199-214.

Fabry, F., C. Frush, I. Zawadzki, and A. Kilambi, 1997: On the extraction of near-surface index of refraction using radar phase measurements from ground targets. J. Atmos. Oceanic Technol., 14, 978-987.

Hu, M., 2005: 3DVAR and cloud analysis with WSR-88D level-II data for the prediction of tornadic thunderstorms, Ph. D. Dissertation, School of Meteorology, University of Oklahoma, 217 pp.

PUBLICATIONS

T.-Y. Yu, R. Reinoso-Rondinel and R. D. Palmer, 2008: Investigation of Non-Gaussian Doppler Spectra Observed by Weather Radar in a Tornadic Supercell, J. Atmos. Oceanic Technol. [in press, referred].

B. L. Cheong, R. D. Palmer, M. Xue, 2008: A Time-Series Weather Radar Simulator Based on High-Resolution Atmospheric Models, Journal of Atmospheric and Oceanic Technology, 25, 230-243, 2008 [published, referred].

B. L. Cheong, R. D. Palmer, C. Curtis, T.-Y. Yu, D. S. Zrnic, D. Forsyth, 2008: Refractivity Retrieval Using the Phased Array Radar: First Results and Potential for Multi-Mission Operation, IEEE Transactions on Geoscience and Remote Sensing, 46(9), 2527-2537 [published, referred].

K. Le, R. D. Palmer, B. L. Cheong, T.-Y. Yu, G. Zhang, S. Torres, 2008: On the Use of Auxiliary Receive Channels for Clutter Mitigation on Phased Array Weather Radar, IEEE Transactions on Geoscience and Remote Sensing, [in press, referred].

K. D. Le, R. D. Palmer, B. L. Cheong, T.-Y. Yu, G. Zhang, and S. M. Torres, Novel Adaptive Beamforming Techniques for Atmospheric Imaging Radars, Amer. Met. Soc. 88th Annual Meeting, New Orleans, LA, January 20-24, 2008 [nonreferred].

Mark Yeary, R. Palmer, M. Xue, T.-Y. Yu, G. Zhang, A. Zahrai, J. Crain, Y. Zhang, R. Doviak, Q. Xu, P. Chilson, Development of a Multi-Channel Receiver for the Realization Multi-Mission Capabilities at the National Weather Radar Testbed, Amer. Met. Soc. 88th Annual Meeting, New Orleans, LA, January 20-24, 2008 [nonreferred].

M. Yeary, T.-Y. Yu, R. Palmer, M. Biggerstaff, D. Fink, and C. Ahern, A Progress Report on a Hands-On Interdisciplinary Program for Severe Weather and Next-Generation Multi-Function Radar, Proceedings of the ASEE Annual Conference, Pittsburgh, Pennsylvania, June, 2008 [nonreferred].

T. Lei, M. Xue, T.-Y. Yu and M. S. Teshiba: Impact of Spatial Over-sampling by Phase-Array Radar on Convective-Storm Analysis using Ensemble Kalman Filter, Amer. Met. Soc. 88th Annual Meeting, New Orleans, LA, January 20-24, 2008 [nonreferred].

M. S. Teshiba, T.-Y. Yu, G. E. Crain and M. Xue: Application of a monopulse phased array system to weather observations for detecting azimuthal shear at sub-beamwidth resolution, Amer. Met. Soc. 88th Annual Meeting, New Orleans, LA, January 20-24, 2008 [nonreferred].

T. Lei, M. Xue and T.-Y. Yu, 2009: Multi-scale Analysis and Prediction of the 8 May 2003 Oklahoma City Tornadic Supercell Storm Assimilating Radar and Surface Network Data using EnKF, Amer. Met. Soc. 89th Meeting, Phoenix, AZ, January 11-15 [accepted, nonreferred].

R. Reinoso-Rondinel and T.-Y. Yu, 2009, Scheduling of the multifunction Phased-Array Radar for adaptive sensing using time balance, Amer. Met. Soc. 89th Meeting, Phoenix, AZ, January 11-15 [accepted, nonreferred].

Y. Umemoto, T. Lei, T.-Y. Yu and M. Xue, 2009, Observation error modeling and EnKF OSSEs examining the impact of spatial and temporal resolution and errors for Phased-Array Radar, Amer. Met. Soc. 89th Meeting, Phoenix, AZ, January 11-15 [accepted, nonreferred].

M. Yeary, R. Palmer, G. Zhang, M. Xue, T.-Y. Yu, A. Zahrai, J. Crain, Y. Zhang, R. Doviak, Q. Xu, and P. Chilson, 2009, An update on multi-channel receiver development for the realization multi-mission capabilities at the National Weather Radar Testbed, Amer. Met. Soc. 89th Meeting, Phoenix, AZ, January 11-15 [accepted, nonreferred].

B. Root, M. Yeary, and T.-Y. Yu, 2009: Consistent clustering of radar reflectivities using strong-point analysis -- a prelude to storm tracking, Amer. Met. Soc. 89th Meeting, Phoenix, AZ, January 11-15 [accepted, nonreferred].